

EVIDENCE FOR BEAMING OF JUPITER'S DECAMETRIC RADIATION: SIMULTANEOUS OBSERVATIONS FROM VOYAGERS AND GROUND-BASED OBSERVATORIES

Koiti Maeda¹ and Thomas D. Carr²

¹*Department of Physics, Hyogo College of Medicine
Nishinomiya, Hyogo 663, Japan*

²*Department of Astronomy, University of Florida
Gainesville, Florida 32611, USA*

Abstract

We present incontrovertible evidence for the beaming of the Jovian decametric radiation, based on simultaneous observations at about 22 MHz from one or both of the Voyager spacecraft and one or the other of two ground-based observatories. We use our data to test the hollow-cone beaming models that have been proposed to account both for the long term statistics of the ground-based observations and for the arc structures discovered in the dynamic spectral plots of Voyager data. We conclude that occurrences of non-Io-related Source A events are determined by the corotation with the inner Jovian magnetosphere of curved-sheet beams, and those of Io-related Source B storms by a similar type of beam that moves with the northern foot of the Io flux tube. Both types of beam can be approximated by hollow-cone beam sectors. We have been able to make rough measurements of the observed portions of some of the beams.

1. Introduction

One of the outstanding features of Jovian decametric radiation is beaming of the radiation. Long-term ground-based observations revealed that the occurrence probability of the noise storm at a given frequency is a joint function of the System III (1965) longitude of the central meridian (CML) and the orbital position of the innermost Galilean satellite, Io, relative to the observer (Io phase). There are three well-defined zones of CML within which the occurrence probability is relatively high. They are called Sources B, A, and C with increasing longitude, according to the classification by Carr et al. (1983). Each component is sub-divided into Io-related and Io-unrelated components. Other Io-related components, i.e., Io-related Sources D and A', were also recognized through broad-band observations by Voyagers (see, for example, Carr et al., 1983). The occurrence probability of each Io-related component correlates strongly with Io phase. The Jovicentric declination of Earth, D_E , changes between $\pm 3.3^\circ$ over the orbital period of Jupiter, 11.9 yr. This slight change in D_E is enough to cause discernible effects in occurrence probability of the Jovian decametric storm (Gulkis and Carr, 1966; Carr et al., 1970; Register and Smith, 1969; Lecacheux, 1974; Thieman et al., 1975; Bozyan and Douglas, 1976). Carr et al. (1970) derived the beam structure, in a statistical sense, of the Source A radiation based

on the D_E dependence of the occurrence probability curve as a function of longitude. Since many statistical results from ground-based observations imply that the Jovian decametric radiation is emitted into beams, it is important to find direct evidence for the beaming of single events.

Dulk (1967) introduced a hollow cone beaming model to account for the Io-related Sources A (Io-A) and B (Io-B), and achieved some success with the model. The basic elements of the Dulk hollow-cone beam model have also been used by others with limited success in modeling the Io-related sources (Goldreich and Lynden-Bell, 1969; Thieman and Smith, 1979; Hashimoto and Goldstein, 1983; Wang, 1985) and in accounting for arc structures in the dynamic spectra obtained by the Voyagers (Warwick et al., 1979a; Pearce, 1981; Goldstein and Thieman, 1981; Staelin, 1981). In this paper we present direct evidence for beaming of the radiation of Io-B and Io-unrelated Source A (non-Io-A) based on simultaneous observations from two Voyager spacecraft and ground-based observatories (the Mizuho-cho Radio Observatory in Japan and the University of Florida Radio Observatory). We demonstrate that the beam associated with each such event can be approximated by a sector of a hollow cone.

2. Multi-station observations

In order to obtain direct evidence for the beaming of Jovian decametric radiation it is necessary to make simultaneous observations from stations which are in substantially different directions as viewed from Jupiter. The first attempt to make such observations was reported by Poquerusse and Lecacheux (1978). They observed two predicted Io-B storms at 30 MHz from the Soviet spacecraft Mars 7 and the Nançay Observatory, and detected Jovian storm activity only at one station in the first case and only at the other station in the second case. This result was interpreted as indicating a beam width less than about 15° separation between the two stations, but it is not clear why the rotation of the planet did not cause the beam to sweep across both stations.

We report on several instances in early 1979 in which simultaneous observations were made at about 22 MHz from the two Voyager spacecraft and a ground-based observatory. The first such instance was in the period from late January to early February, 1979; the ground station was the Mizuho-cho Radio Observatory in Japan. The directions of the three stations in early February, 1979, as viewed from Jupiter, are indicated in Figure 1. In this case, the angle between Voyager 1 and Earth direction was about 23° , and that between Earth and Voyager 2 directions was about 29° . Part of our analysis of this instance has been already reported (Maeda and Carr, 1984). In another instance the ground station was the University of Florida Radio Observatory. Figure 2 indicates the declinations of Voyager 1, Voyager 2, and Earth as a function of day of year, 1979. It is apparent that the Voyager observations greatly extended the declination range over which the Jovian radiation had been observed from Earth.

The sensitivities of the ground-station radiometers were on the order of $10^{-22} \text{Wm}^{-2} \text{Hz}^{-1}$. Since the distance from Jupiter to Voyager 1 changed relatively rapidly in the observation period, the detection sensitivity of the Voyager 1 receiver also changed. The detection

sensitivity of Voyager 1, adjusted to Earth distance, was approximately the same as those of the ground stations in the period from late January to early February, 1979.

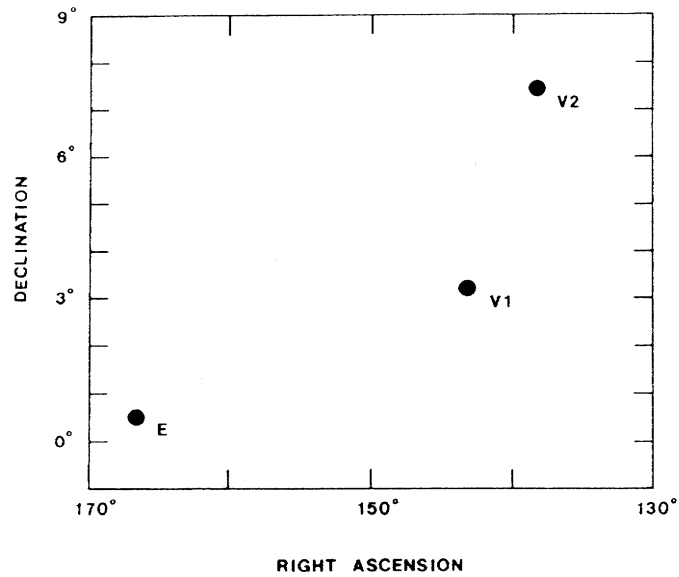


Fig. 1: Relative positions of Voyager 1, Voyager 2, and Earth in early February, 1979, in the Jovicentric sidereal coordinates.

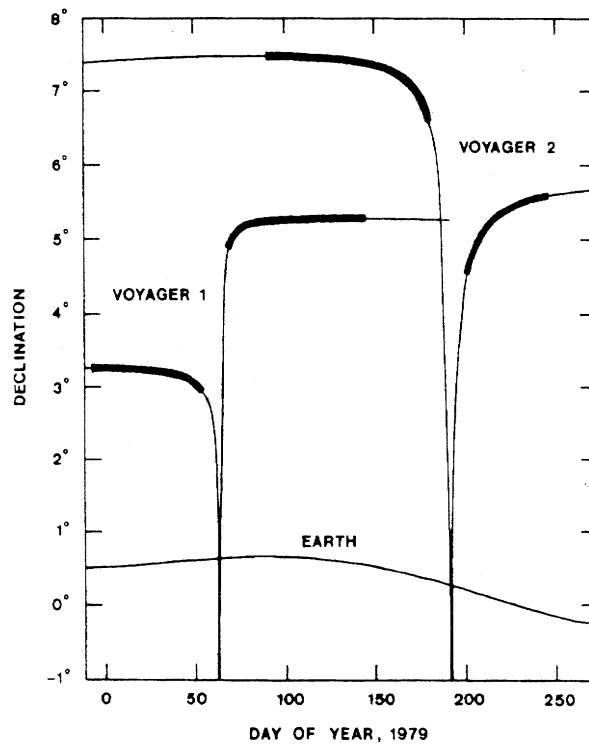


Fig. 2: Jovicentric declinations of Voyager 1, Voyager 2, and Earth as a function of day of year, 1979. Data in the periods indicated by the thick solid curves are used for an occurrence-probability analysis of the Io-B radiation.

3. Comparison of ground-based and spacecraft data

Observations at Mizuho-cho were made at 21.86 MHz. Each of the Mizuho-cho storms was compared with the Voyager 1 channel 63 (21.811 MHz) data, as in Figure 3. In order to represent the Mizuho-cho chart-recorder data compactly in the figure, bursts of emission are represented by triangles, each of which indicates schematically the starting and ending times of a burst and the relative peak intensity. As seen in this figure, strong Io-B emissions were observed at Mizuho-cho, but only weak ones with a short duration were observed at Voyager 1. On the other hand, the non-Io-A storm was well correlated at Voyager 1 and Mizuho-cho. The Mizuho-cho storms which we were able to identify in the recording from Voyager 1 were classified into two groups, one well correlated and the other poorly correlated. These Mizuho-cho storms are plotted in the CML vs. Io phase plane in Figure 4. The solid and dashed lines in this figure indicate the well-correlated and poorly-correlated storms, respectively. It is apparent that correlated storms were essentially of type non-Io-A. On the other hand, no correlated storms were found in the Io-B region. The behavior of the Io-B beam is completely different from that of the non-Io-A beam.

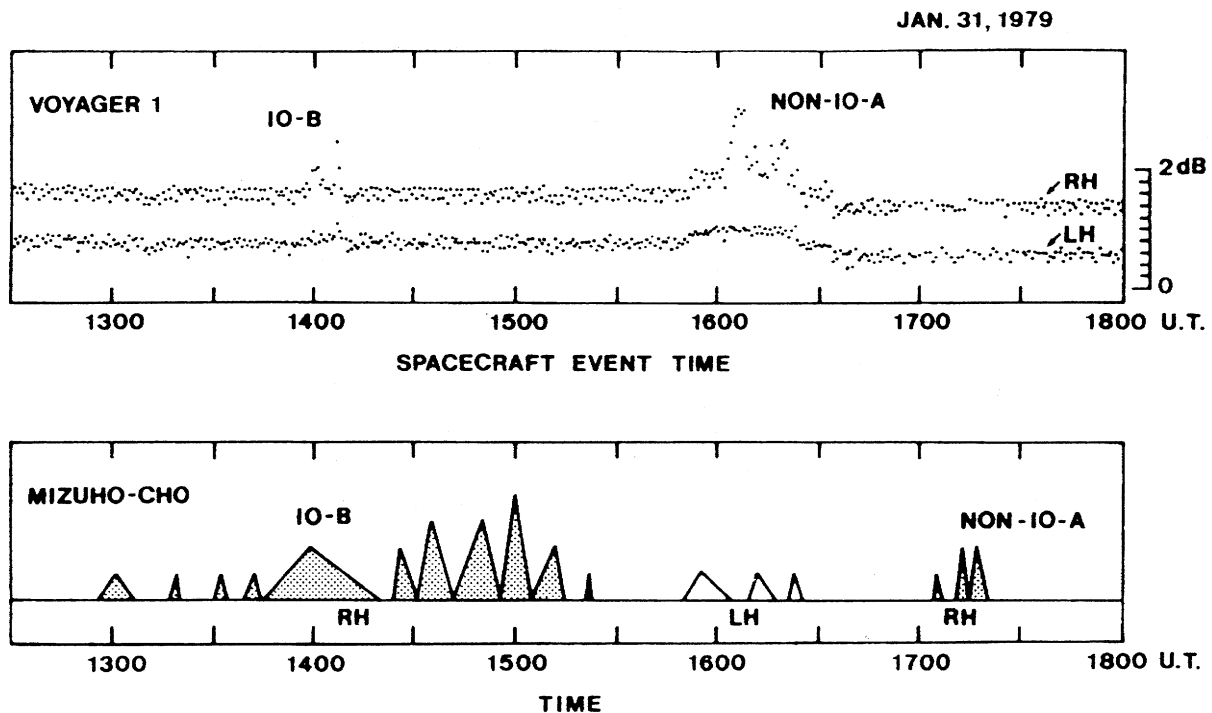


Fig. 3: Comparison of the recording from Voyager 1 channel 63 (21.811 MHz) and the 21.86 MHz observations at the Mizuho-cho Radio Observatory in Japan. The right-hand (RH) and left-hand (LH) components from Voyager 1 channel 63 are plotted as a function of time on a logarithmic scale. The Mizuho-cho record is represented schematically by triangles, each of which indicates the starting time, the ending time, and the relative peak intensity of a burst of emission.

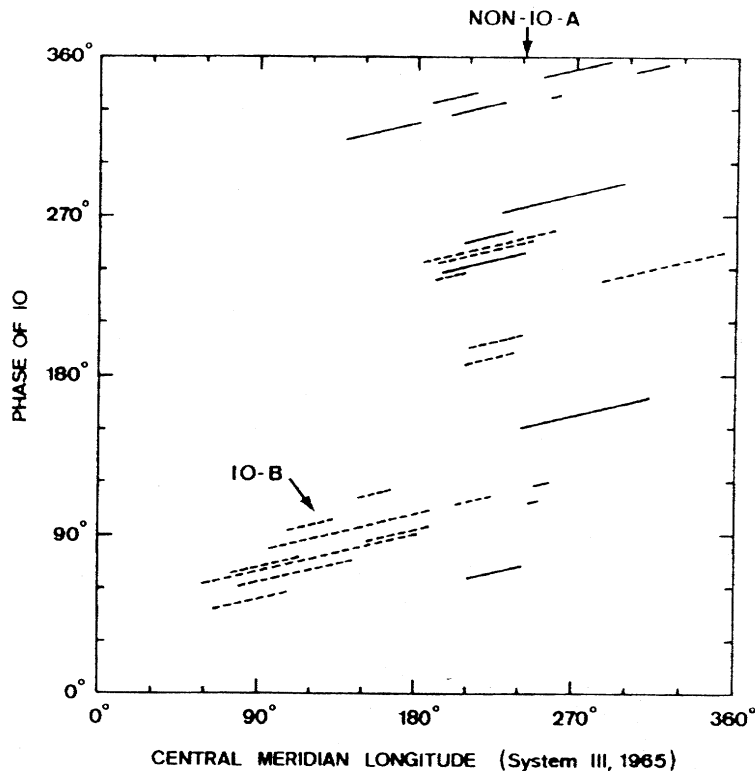


Fig. 4: Mizuho-cho storms that were identified in the recordings from Voyager 1. The solid lines indicate the storms that were correlated at Voyager 1 and Mizuho-cho, and the dashed lines represent the poorly correlated storms.

4. Beam structure of non-Io-A radiation

We investigated the non-Io-A beam structure using the correlated-storm data, an example which is shown in Figure 5. Figure 5a represents the 21.86 MHz interferometer and polarization records at Mizuho-cho. Figure 5b indicates the right-hand intensity component from the Voyager 1 channel 63 (21.811 MHz) on a logarithmic scale. We can see spiky bursts in the Mizuho-cho record, which were presumably caused by interplanetary and ionospheric scintillation. We can also see a set of four spiky-burst groups, each of which had a duration of about 10 min. The corresponding Voyager 1 record shows a similar set of four long bursts without fine structure seen in the Mizuho-cho record. We believe that this observed correlation indicates that non-Io-A radiation is emitted in quasi-continuous beams that corotate with the planet, and that the spikiness of the Mizuho-cho record is due to scintillation in the terrestrial ionosphere and in the relatively long interplanetary propagation path.

To derive the beam structure of the non-Io-A radiation we analyzed starting and ending times of the correlated storms. To minimize the effect of the detection sensitivity change of the spacecraft we selected five correlated storms that were observed in a relatively short period from January 31 through February 10. We assumed that each correlated storm was caused by the sweeping past the observer of a quasi-continuous beam that corotates with Jovian inner magnetosphere at the System III angular velocity. For the storm shown in Figure 5 we used starting and ending times of the well-defined main body of the storm.

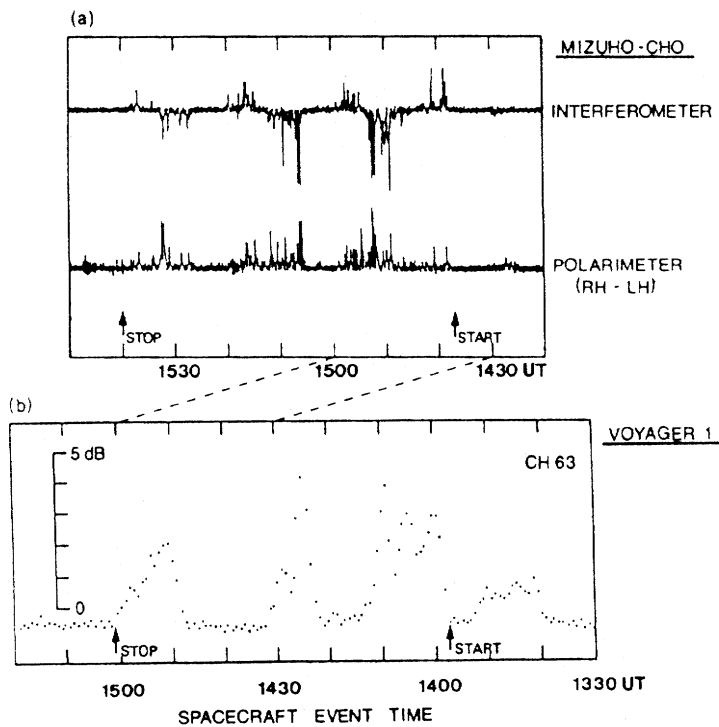


Fig. 5: Correlated storm on February 3, 1979, as observed at Voyager 1 and Mizuho-cho. The 21.86 MHz polarization and interferometer records at Mizuho-cho (a), and the recording from the Voyager 1 channel 63 (21.811 MHz) (b) are shown. The starting and ending times of the well-correlated main body of the storm are indicated by the arrows.

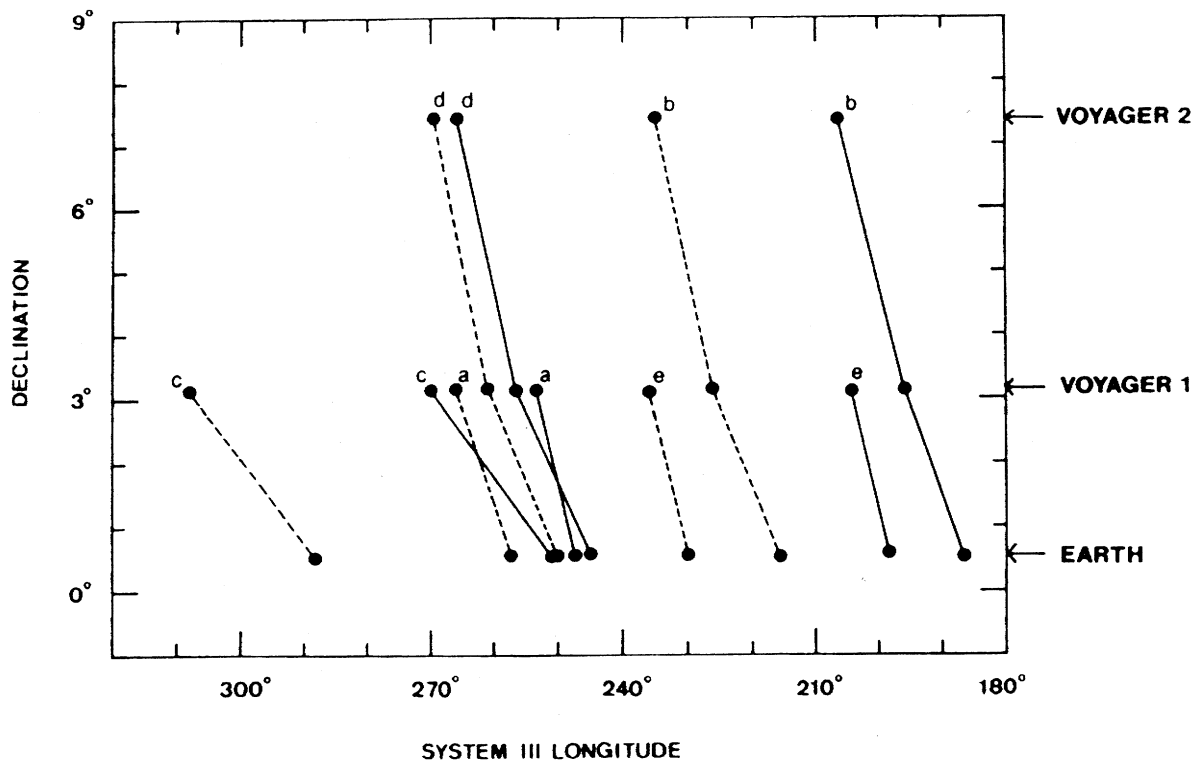


Fig. 6: Storm envelope beam structure of non-Io-A radiation, projected onto the corotating celestial sphere on which the coordinates are Jovicentric declination and System III longitude. Solid lines connect points indicating station positions at the starting times of a storm that was correlated at two or three stations, and dashed lines designated by the same letter at the top connect the ending points of the same storm.

In order to specify the radiation direction we can use projections onto the corotating celestial sphere on which the coordinates are Jovicentric declination and System III longitude. Each starting or ending time was converted to the CML as viewed from the corresponding station. This CML represents the longitude which faced Earth at the instant at which the observed radiation left Jupiter. The direction of the observed radiation is represented by a point on the corotating celestial sphere at a longitude equal to this CML and at the declination of the corresponding station. The results from such analyses of the five correlated storms are shown in Figure 6. The solid and dashed lines labeled with the same letter indicate the leading and trailing boundaries of a storm emission beam. As seen in this figure the leading and trailing boundaries of a storm emission beam are nearly parallel to each other and to those of the other. This is consistent with a model in which each storm emission beam is in the form of a thick sheet. The results from the three-station data indicate that each sheet is somewhat curved. This is consistent with the hollow-cone beam model. If each beam were a full hollow cone there would have been another active longitude preceding the non-Io-A longitude zone. A search revealed no such image source. It is therefore concluded that each beam can be approximated by a sector of a hollow cone.

We can calculate the cone half-angles for the four three-station data sets in Figure 6. The estimated values are 35° , 40° , 41° , and 58° , the average being 44° . Dulk originally assumed that Sources Io-B and Io-A resulted from the Earth-alignment of opposite limbs of the same hollow cone beam. Our 44° cone half-angles, however, are much too small to account for non-Io-B as the other limb of the non-Io-A cone. It is therefore necessary to postulate that only a restricted sector of a hollow cone is responsible for non-Io-A. The beam structure that we have found is thus fundamentally different from that of the Dulk model.

5. Beaming of Io-B radiation

5.1 Occurrence-probability analysis of the 21.8 MHz Io-B emissions observed by Voyagers

An analysis of Io-B occurrence probability as a function of CML and Io phase at about 21.8 MHz (channel 63) was made from three sets of Voyager data. The observation periods and spacecraft declination ranges for the three data sets are indicated in Table 1 and Figure 2. It is apparent that the Voyager data considerably extend the declination range attainable from Earth.

Occurrence probability was calculated for each 5° by 5° area element in the CML-Io phase plane. Smoothing of the occurrence probabilities was made over 4 area elements at a time by weighting in the proportions 1:3:3:1 in the vertical direction first, then by the same weighting function in the horizontal direction. The results are shown in Figures 7a, 7b, and 7c. In each figure the 30% and 60% contours are indicated. Figure 7d shows the 30% contour for the aggregate of the data of Figures 7a, 7b, and 7c. A necessary condition for the occurrence of Io-B storms is thus that the points indicating the CML and Io phase lie inside this contour. The three inclined-dashed lines in Figure 7d indicate the loci of

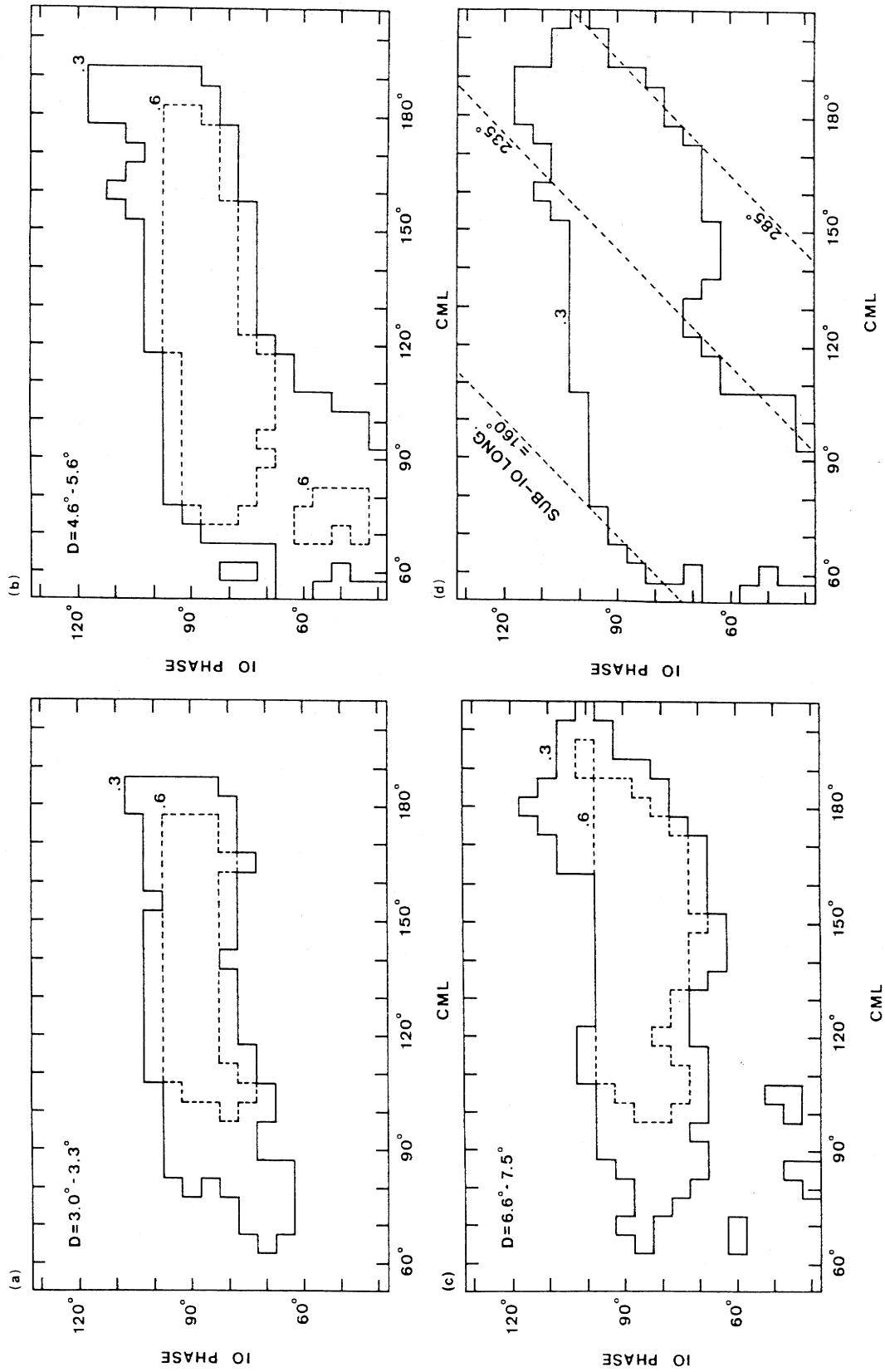


Fig. 7: Io-B occurrence-probability contours (30% and 60%) in CML vs. IO phase plane for three data sets: a) Voyager 1 data in the pre-encounter period, b) Voyager 1 data in the post-encounter period, and c) Voyager 2 data in the pre-encounter period. The range of station declination (D) for each data set is indicated. The fourth plot (d) is the 30% contour for the aggregate of the data in the three sets.

points having fixed sub-Io longitudes of 160° , 235° , and 285° , respectively. It can be seen that the Io-B storms occur in a sub-Io longitude range from 160° to 285° . It appears that the directivity of the Io-B beam changes at a sub-Io longitude of about 235° . This may be caused by a change in interaction between Io and the Io torus.

Table 1:

Data Sets Used for Io-B Occurrence-Probability Analysis			
	Period	Declination Range	
1. Voyager 1	Dec.25, 1978 to Feb.21, 1979	3.0° to 3.3°	
2. Voyager 1	Mar.10 to May 25, 1979	4.6° to 5.6°	
Voyager 2	July 21 to Sept.3,1979		
3. Voyager 2	Apr.1 to June 30, 1979	6.6° to 7.5°	

5.2 Evidence for beaming of Io-B radiation

Figure 8 shows an example of simultaneous observations of an Io-B storm from Voyager 1 and Mizuho-cho. Spacecraft Event Time means the Universal Time (UT) as observed at the spacecraft. In Figure 9, the same Io-B storm is plotted as intensity vs. sub-Io longitude at the instant at which the observed radiation left the planet. The use of sub-Io longitude at the instant of departure instead of at the time of signal reception eliminates the effect of the difference in propagation times from Jupiter to Voyager 1 and Earth. If we accept the fact that Io-B radiation is produced when the sub-Io point lies within a particular range of Jovian longitude, then Figure 9 gives us clear evidence for relatively narrow beaming of the radiation, for the following reason. It is seen in the figure that the strongest emission toward Earth occurred when the sub-Io longitude was in the vicinity of 260° , but within the same span of time no radiation was emitted toward Voyager 1. Therefore the radiation must have been restricted to a beam that was sufficiently narrow to exclude radiation from the direction of Voyager 1 when it was near maximum in the direction of Earth. At other sub-Io longitudes (in the same figure) for which some radiation was emitted toward both Earth and Voyager 1, the beam maximum probably lay between the directions of the two stations, and the beamwidth was sufficient that neither was completely excluded from the beam.

In Figure 10, the February 7 storm is plotted on the CML vs. Io-phase plane together with the 30% and 60% occurrence-probability contours of Figure 7a. In this figure the observing track for each station is indicated by the inclined solid line and the emission bursts are represented by the triangles. This figure accounts for the above-mentioned lack of the Voyager 1 counterpart of the strong Mizuho-cho storm. The 260° sub-Io longitude line is shown by the dashed line. Around the 260° sub-Io longitude, the observation line of Earth was within the 30% contour, while that of Voyager 1 was outside of the 30% contour. We found many such examples. These results therefore indicate that the shape

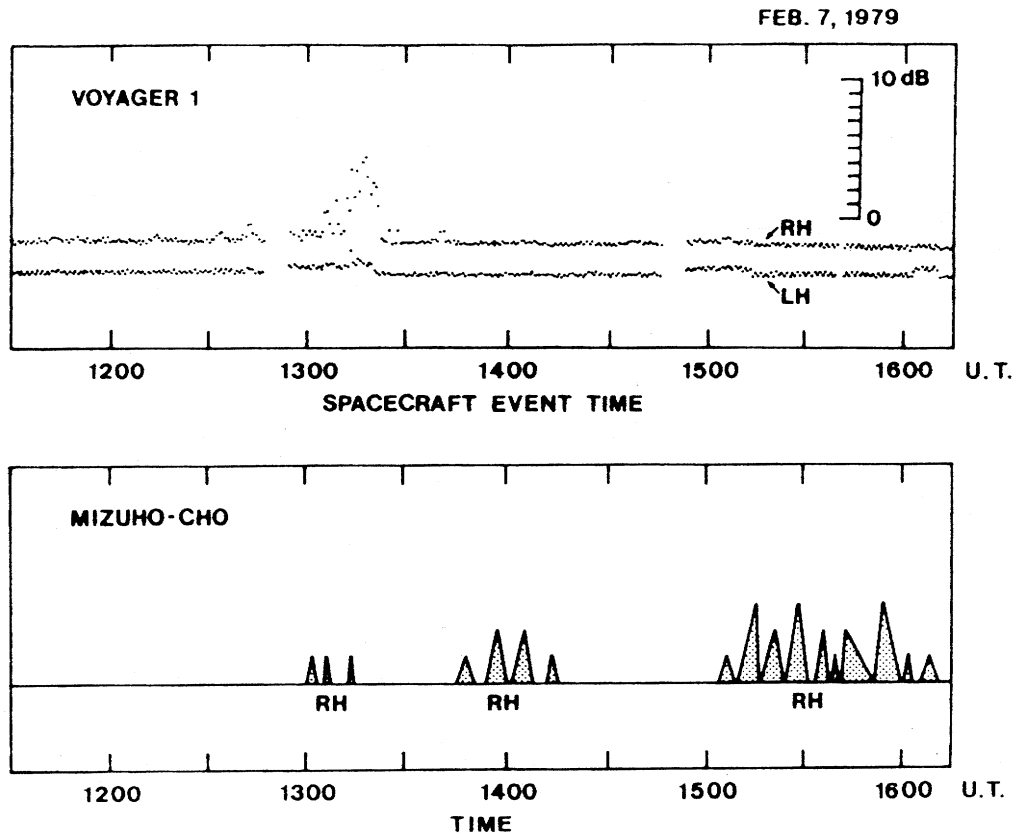


Fig. 8: Simultaneous observations of an Io-B storm on February 7, 1979 from Voyager 1 and the Mizuho-cho Radio Observatory. The intensities versus time plot of the recording from Voyager 1 channel 63 (21.811 MHz) is shown on a logarithmic scale at the top. At the bottom the 21.86 MHz Mizuho-cho storm is represented schematically using triangles, each of which indicates the starting time, the ending time, and the relative peak intensity of a burst.

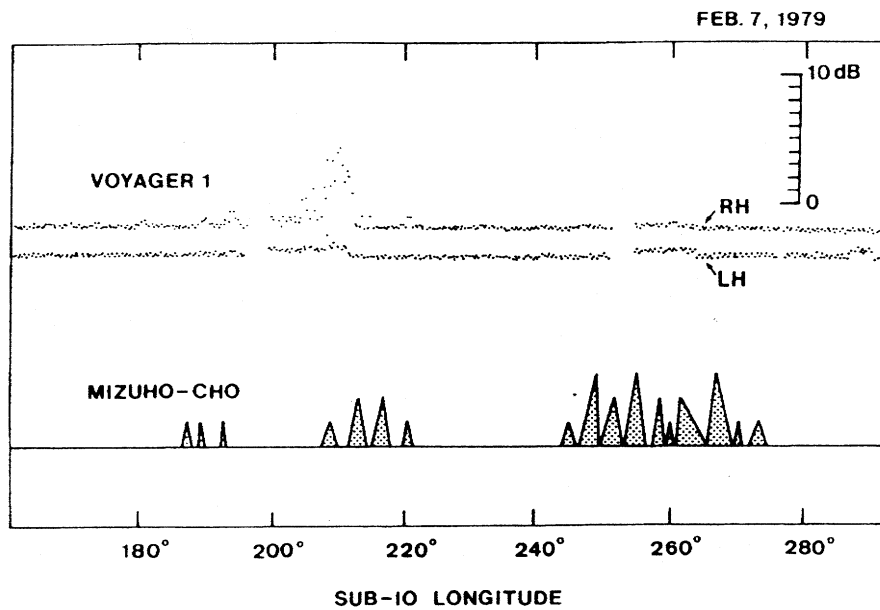


Fig. 9: The same storm observations as indicated in Figure 8, but plotted as a function of sub-Io longitude.

of the Io–B region in the CML vs. Io phase plane results basically from the beaming of the Io–B radiation.

5.3 Behavior of the Io–B beam

Two pairs of simultaneous observations from Voyager 1 and the University of Florida Radio Observatory (UFRO) give us further evidence for beaming of the Io–B radiation and also information about the behavior of the Io–B beam. Figure 11 shows the observation lines in the CML vs. Io–phase plane of the two stations on January 19 and February 2, 1979. The line of observation of UFRO (i.e., E in the figure) on January 19 was essentially the same as that of Voyager 1 on February 2. On January 19, UFRO observed a strong Io–B storm but Voyager 1 did not, while on February 2, Voyager 1 observed a strong Io–B storm but UFRO did not. The two Io–B storms were homologous in the sense that the main body of each storm occurred within the shaded part of the observation line in Figure 12. It thus appears that the beam pattern was more or less the same on January 19 and February 2. Our calculations indicate that on January 19 whatever emission there may have been in the direction of Voyager 1 was more than 15 dB below that in the direction of Earth, and on February 2 any emission in the direction of Earth was more than 30 dB below that toward Voyager 1. Figures 12a and 12b illustrate the beaming geometry for two values of sub–Io longitude, 230° and 250° , respectively, as deduced from the two pairs of simultaneous observations from Voyager 1 and UFRO made on January 19 and February 2. Jovian longitude is given by the scale on each of the two large circles. The sub–Io longitudes are indicated by the small filled squares. Emission was observed at the stations CMLs indicated by the small filled circles, but not at those indicated by the small open circles. Each figure therefore indicates that the radiation was emitted into a beam, the direction of which is between the two longitudes indicated by the small open circles. The sub–Io longitude increases with time, because the angular velocity of Jupiter’s rotation is greater than the orbital angular velocity of Io. If the Io–B beam were to corotate with the Jovian inner magnetosphere, the CMLs at which the emissions are observed would remain unchanged. It is apparent from Figures 12a and 12b, however, that the CML at which the emissions were observed, increased with increasing sub–Io longitude. This gives us incontrovertible evidence that the main body of the Io–B beam is moving with the magnetic flux tube connected with Io instead of corotating with the Jovian inner magnetosphere.

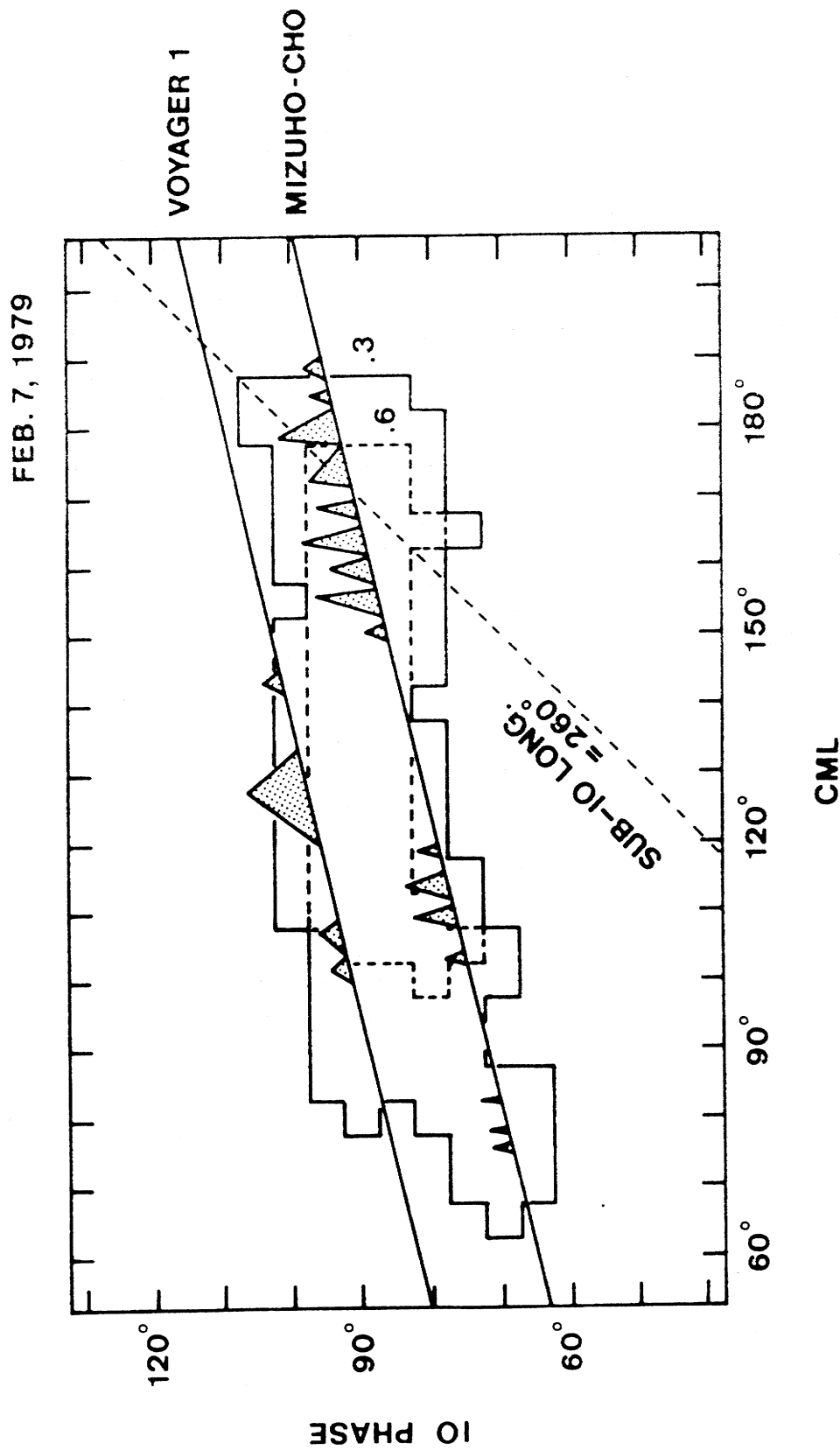


Fig. 10: Comparison of the occurrence-probability plot of Figure 7a and the simultaneous observations of the February 7 Io-B storm from Voyager 1 and Mizuho-cho. Each inclined solid line indicates the line of observation of the corresponding station, and the storm emission bursts are schematically represented by the triangles.

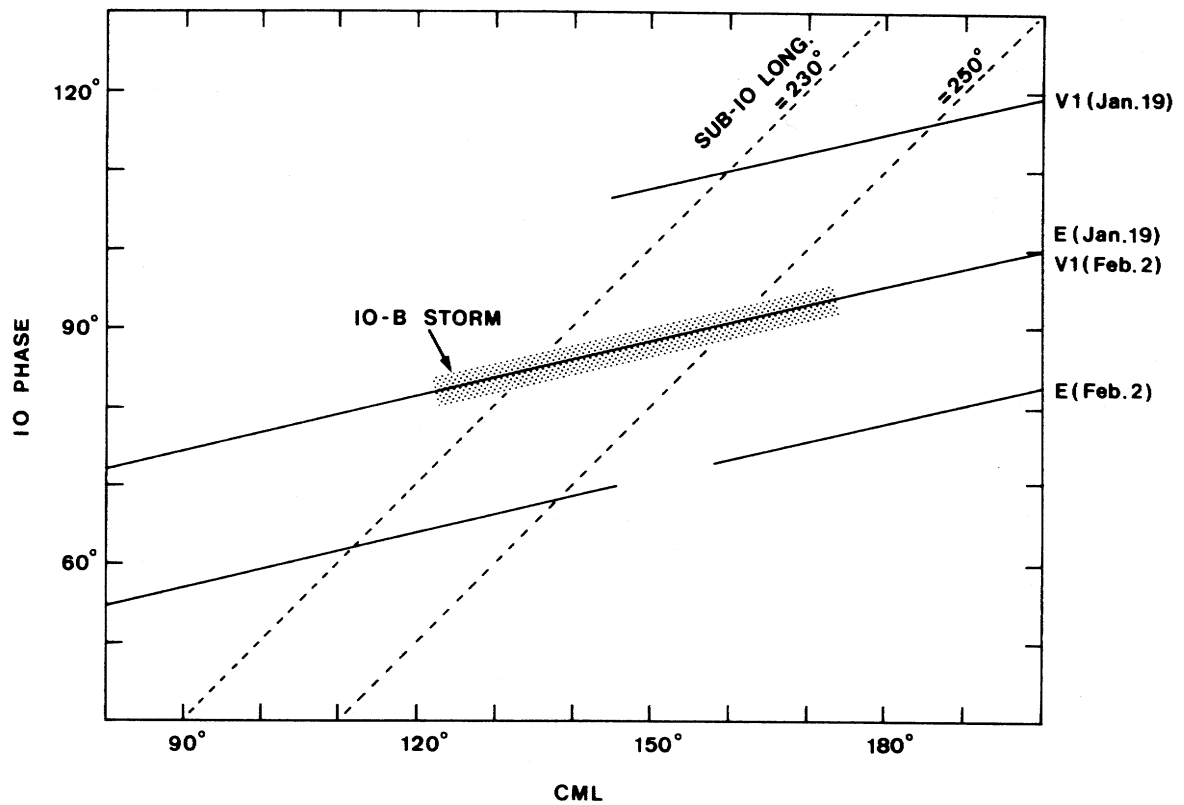


Fig. 11: Tracks on the Io phase-CML plane related to the two Io-B storms that were observed simultaneously from Voyager 1 (V1) and the University of Florida Radio Observatory (Earth station, E). The middle one of the three inclined parallel lines is the time-line for the Earth station during the January 19 observing period, and by fortunate coincidence, also the time-line for the Voyager 1 station during the February 2 observing period. The time lines for Voyager 1 during the January 19 observing period and for Earth during the February 2 observing period are also indicated. The shaded band along the middle time-line covers both the part of the Earth time-line when the January 19 storm was in progress and the Voyager 1 time-line when the February 2 storm was in progress. The two inclined dashed lines represent the loci of points having fixed sub-Io longitudes of 230° and 250° , respectively.

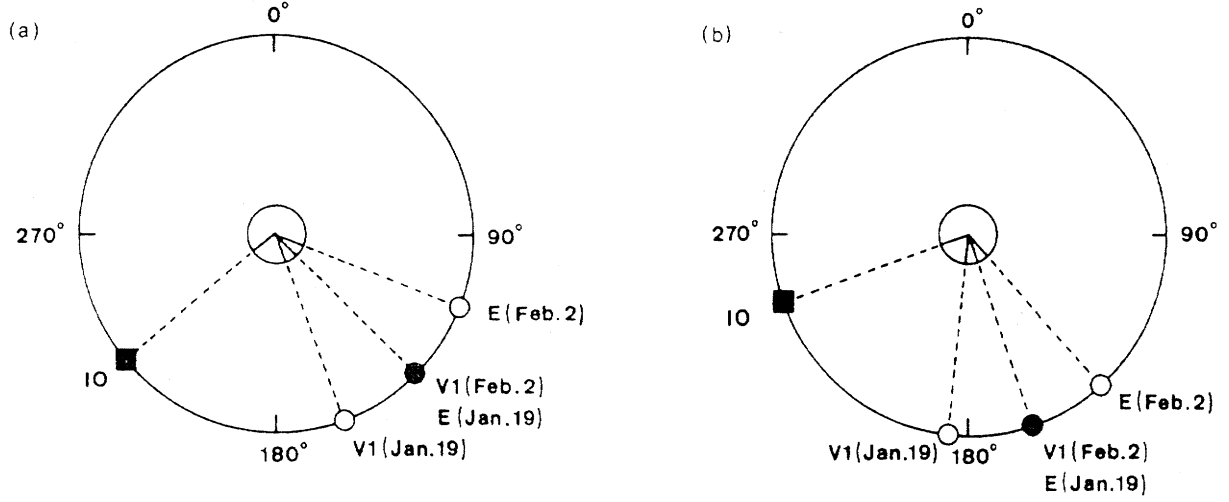


Fig. 12: Longitudinal relationship between the position of Io and the beaming direction of Io-B radiation. In each figure the open and filled circles indicate the CMLs of Voyager 1 (V1) and the University of Florida Radio Observatory (E) for a sub-Io longitude shown by the filled square. The Io-B radiation was received at the CML indicated by the filled circle, but not at the CMLs indicated by the open circles.

5.4 Beam structure of Io-B radiation

Several authors (Bozayan and Douglas, 1976; Lecacheux, 1974; Thieman et al., 1975) showed from long-term ground-based observations that the occurrence-probability profile of the Io-B emissions as a function of Io phase has a D_E dependence; the centroid of Io phase of the occurrence-probability profile decreases with increasing D_E . This observed effect is explainable from the geometry of the Io-B hollow-cone emission beam at the northern foot of the Io flux tube (Desch, 1978). Since Voyager observations were made at declinations higher than those attainable from Earth, it is interesting to investigate the D_E dependence of the Voyager data. We used the same data from which the results presented in Section 5.1 were obtained. We calculated the probability occurrence of activity within the CML range 130° to 140° for each 5° of Io phase, and plotted this occurrence probability as a function of Io phase. Such occurrence-probability curves for three data sets are shown in Figure 13. In each panel the weighted mean value of Io phase is indicated by an arrow as a measure of the centroid of each profile. As seen in Figure 13, the centroid of Io phase decreases with increasing station declination from 3° to 7.5° . This sense is consistent with that obtained from ground-based data. Thus our results further support that the Io-B radiation is emitted in a hollow-cone beam from the northern foot of the Io flux tube.

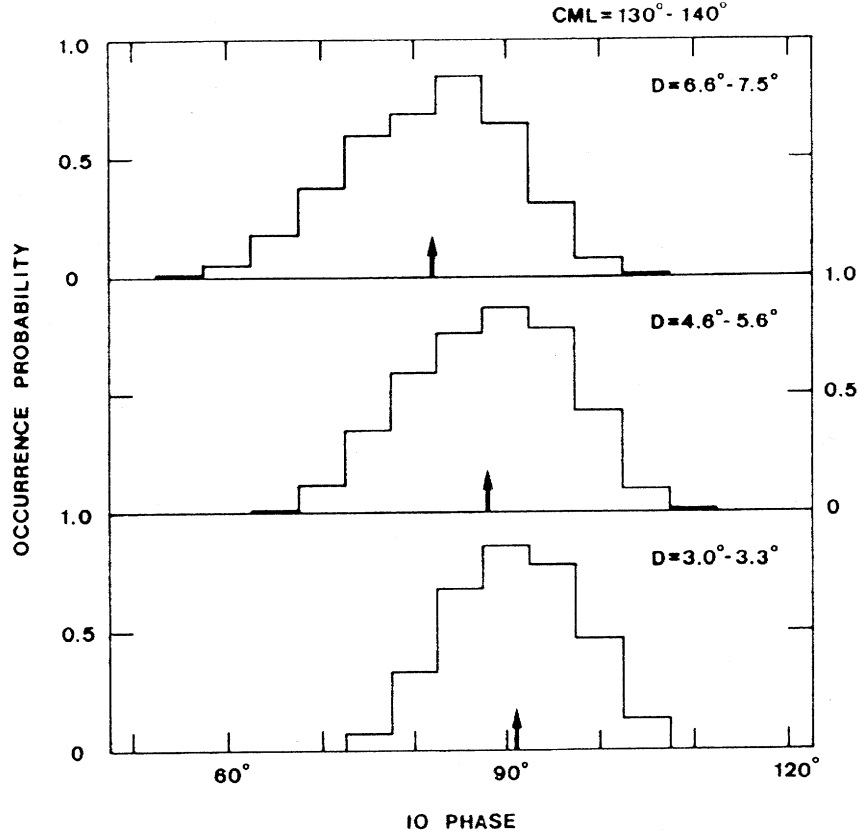


Fig. 13: Occurrence probability profile as a function of Io phase. Each profile was obtained from an analysis of the Voyager 1 and/or Voyager 2 data in the designated declination (D) range. The occurrence probability is the average over the CML range from 130° to 140° . In each panel the weighted mean value of Io phase is indicated by an arrow as a measure of the centroid of Io phase.

In the light of long-term ground-based observations we investigated whether each beam of the Io-dependent radiation can be approximated by a full-hollow cone or just a sector of a hollow cone. Figure 14 shows a 22.2 MHz occurrence probability plot in the sub-Io longitude vs. Io phase plane (taken from Bozyan and Douglas, 1976). In this figure a vertical line gives us information of the beam directivity for a given sub-Io longitude. If the emission beam is a full hollow cone we should find two active zones of Io phase for a given sub-Io longitude. Figure 14 rules out the possibility. The situation is schematically shown for the three representative sub-Io longitudes, i.e., 165° , 240° , and 280° . For a sub-Io longitude of 165° , we find Io-A at Io phases around 240° , but no other active Io-phase zone. The Io-related emissions in this case therefore are emitted in a direction only on the west side of Io, as schematically shown at the bottom of Figure 14. For a sub-Io longitude of 240° , the Io-related beam lies only on the east side of Io (Io-B), and for a sub-Io longitude of 280° , only on the west side of Io (Io-C). These results indicate that each Io-related beam at 22.2 MHz lies basically on either side of the sub-Io longitude. The Io-A and Io-B emissions at 22.2 MHz therefore cannot be attributed to two limbs of the same hollow-cone beam. Since, as we previously mentioned, the Io-B centroid drift in Io phase with station declination supports the hollow-cone beaming we believe that each

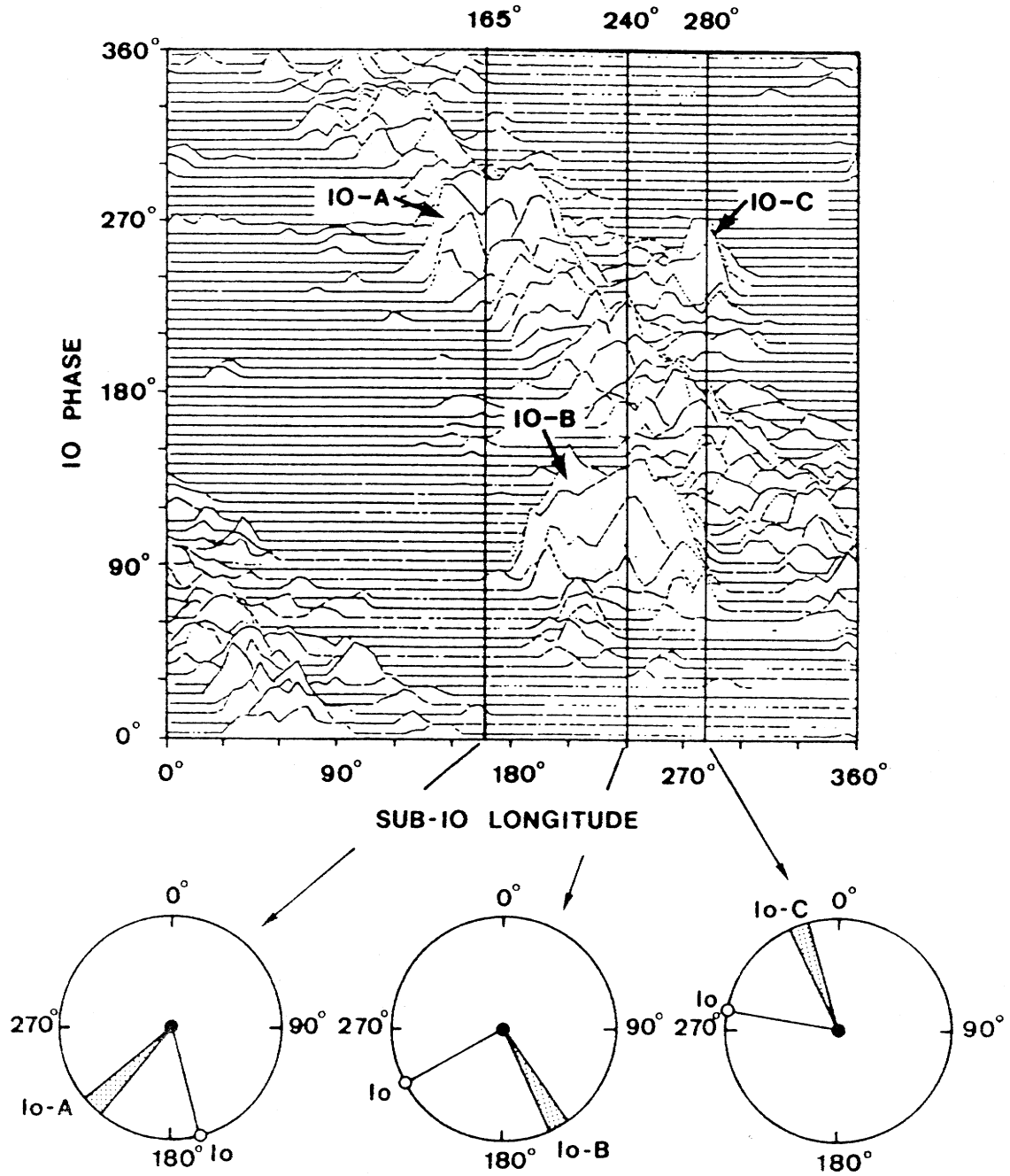


Fig. 14: Beaming of Io-related radiation. The top panel is the 22.2 MHz storm occurrence probability plot for positive D_E (taken from Bozyan and Douglas, 1976). The beaming geometry, i.e., the longitudinal relationship between the position of Io and the Io-related emission beam, is shown schematically for each of three representative sub-Io longitudes at the bottom.

Io-B radiation beam is also approximated by a sector of a hollow cone as the non-Io-A radiation beam is, and that the same is probably true for Io-A and Io-B beams.

6. Conclusion

We have demonstrated that fixed-frequency-observed individual emission events during non-Io-A storms apparently result from the corotation with Jupiter of quasi-continuous beams approximately in the form of sectors of hollow cones. The half-opening angle of each non-Io-A emission cone is approximately 44° at 22 MHz. We have also demonstrated that the main body of the Io-B beam can be approximated by a sector of a hollow cone moving with the Io flux tube, and that beaming in sectors of hollow cones is probably true for Io-A and Io-C radiation. It is not known why the beams are conical sectors rather than full hollow cones; this could be due either to some azimuthal asymmetry in the emission process, or to a subsequent propagation effect. Whatever its cause, the establishing of the conical sector beam structure will provide a valuable new constraint for future theoretical developments. The hollow-cone-sector beam structure of individual events must be reconciled with the Dulk full-hollow-cone beam structure that is apparently responsible for both Io-B and Io-A storm activities as a whole, and also with the hollow-cone beams believed to produce individual dynamic spectral arcs (Warwick et al., 1979a; Pearce, 1981; Goldstein and Thieman, 1981; Staelin, 1981). The first two of these beam types are undoubtedly different. We believe that the Dulk hollow-cone Io-B – Io-A beam represents a global feature, and is the envelope of the sequences of conical sector beams associated with individual emission events within Io-B and Io-A storms. On the other hand, it is possible that the third beam type, that responsible for dynamic spectral arcs, may be the same as the conical-sector beams. Each spectral arc beam is believed to be a hollow cone emitted from an electron cyclotron source, the cone angle being different depending on the source altitude. Our conical-sector beams may simply be fixed-frequency manifestations of the dynamic spectral beams. It may soon be feasible to establish the true relationship between the three beam types from more detailed modeling and comparison with the observational data.

Acknowledgements: We wish to express our thanks to the Voyager Planetary Radio Astronomy team and its associates. This work was partly supported by the National Science Foundation under grant AST 8400208 and by the National Aeronautical and Space Administration under grant NAG 5-773 through Goddard Space Flight Center, both with the University of Florida.

